



Provided by the author(s) and NUI Galway in accordance with publisher policies. Please cite the published version when available.

Title	Optimizing nitrate removal and evaluating pollution swapping trade-offs from laboratory denitrification bioreactors
Author(s)	Healy, Mark G.; Barrett, Maria; Serrenho, Ana
Publication Date	2014-10-29
Publication Information	Healy, M.G., Barrett, M., Lanigan, G., Serrenho, A., Ibrahim, T.G., Thornton, S.F., Rolfe, S.A., Huang, W.E., Fenton, O. (2014) 'Optimizing nitrate removal and evaluating pollution swapping trade-offs from laboratory denitrification bioreactors'. <i>Ecological Engineering</i> , 74 :290-301.
Publisher	Elsevier
Link to publisher's version	http://dx.doi.org/10.1016/j.ecoleng.2014.10.005
Item record	http://hdl.handle.net/10379/4723

Downloaded 2019-01-23T01:36:24Z

Some rights reserved. For more information, please see the item record link above.



1 *Published as: Healy, M.G., Barrett, M., Lanigan, G., Serrenho, A., Ibrahim, T.G.,*
2 *Thornton, S.F., Rolfe, S.A., Huang, W.E., Fenton, O. 2014. Optimizing nitrate removal and*
3 *evaluating pollution swapping trade-offs from laboratory denitrification bioreactors.*
4 *Ecological Engineering 74: 290 – 301. <http://dx.doi.org/10.1016/j.ecoleng.2014.10.005>*
5

6 **Optimizing Nitrate Removal and Evaluating Pollution Swapping Trade-Offs**
7 **From Laboratory Denitrification Bioreactors**
8

9 M.G. Healy^a, M. Barrett^b, G. Lanigan^c, A. Serrenho^a, T.G. Ibrahim^c, S.F. Thornton^d,
10 S.A. Rolfe^e, W.E. Huang^f, O. Fenton^{c*}
11

12 ^aCivil Engineering, National University of Ireland, Galway, Co. Galway, Rep. of
13 Ireland.

14 ^bMicrobiology, National University of Ireland, Galway, Co. Galway, Rep. of Ireland.

15 ^cTeagasc, Johnstown Castle, Environment Research Centre, Co Wexford, Rep. of
16 Ireland

17 ^dGroundwater Protection and Restoration Group, Kroto Research Institute, University
18 of Sheffield, UK.

19 ^eDepartment of Animal and Plant Sciences, University of Sheffield, UK.

20 ^fKroto Research Institute, University of Sheffield, UK.

21
22 *Corresponding author. Tel: +353 539171271; fax: +353 53 9171271. E-mail address:
23 owen.fenton@teagasc.ie
24

25 **Abstract**
26

27 Denitrification bioreactors, typically containing woodchips, are artificial sinks used to
28 remediate nitrate (NO_3^-) losses on agricultural landscapes. Analysis of these
29 bioreactors frequently considers their efficacy in terms of only a single contaminant
30 (for example, NO_3^-), but does not consider other losses – ammonium (NH_4^+),

31 phosphorus (PO_4^{3-}), methane (CH_4), carbon dioxide (CO_2) and nitrous oxide (N_2O). In
32 this study, laboratory-scale denitrifying bioreactors operated at hydraulic retention
33 times (HRTs) ranging from 4 to 22 d, containing either lodgepole pine woodchips
34 (LPW), lodgepole pine needles (LPN), barley straw (BBS) or cardboard, were
35 investigated to elucidate operational optima considering three scenarios using: (1)
36 only NO_3^- net fluxes (2) NO_3^- , NH_4^+ and PO_4^{3-} combined fluxes (3) all fluxes (water
37 and gaseous) combined. At the end of the experiment, after up to 745 days of
38 operation, the bioreactors were destructively sampled for microbial analysis. In
39 Scenario 1, there was a net removal in the bioreactors, which generally performed
40 best at shorter HRTs. In Scenario 2, there was a net release of contaminants from all
41 bioreactors, which substantially increased in Scenario 3. Total greenhouse gas
42 emissions were highest for the cardboard bioreactors ($296 \text{ g CO}_2\text{-eq m}^{-2} \text{ d}^{-1}$) at the
43 longest HRT, and were dominated by CH_4 emissions. Highest N_2O emissions
44 emanated from LPN and LPW bioreactors, which also had a greater proportion of
45 denitrifiers than the other bioreactors. Overall, considering all three scenarios, LPN
46 bioreactors were the best performing at all HRTs. However, the long-term availability
47 of its carbon source may be limited, as there was an 80% reduction over a 560 d
48 period.

49

50 *Keywords:* Denitrification; denitrification bioreactors; greenhouse gas emissions;
51 pollution swapping.

52

53 **1. Introduction**

54

55 Excess reactive nitrogen, such as nitrate (NO_3^-), ammonium (NH_4^+) or nitrous oxide
56 (N_2O) are now at levels which contribute to eutrophication of terrestrial and aquatic
57 ecosystems (Flecharth *et al.*, 2011) and climate change (Richardson *et al.*, 2009). In
58 Europe, nitrogen (N) concentrations in rivers, lakes, aquifers and coastal regions are
59 high in some regions, and groundwater NO_3^- concentrations are generally on the
60 increase (Grizzetti *et al.*, 2012). Residence times of pollutants migrating through soil,
61 subsoil and aquifers can be from months (e.g. well drained and high permeability) to
62 years (e.g. moderately drained and low permeability) (Fenton *et al.*, 2011), leading to
63 sustained losses of NO_3^- to surface water and indirect N_2O emissions to the
64 atmosphere in areas where only partial denitrification occurs (e.g. areas of high water
65 velocity, high dissolved oxygen (DO) concentrations, or low dissolved organic carbon
66 (DOC) concentrations; Durand *et al.*, 2011). The carbon (C) and N cycles are
67 intrinsically linked and depend heavily on the dynamic development of in situ
68 microbial communities, which transform these communities via different pathways.

69

70 Denitrification bioreactors containing organic C rich media, located where
71 denitrification potentials are low and NO_3^- concentrations are high (e.g. drainage tiles
72 or outlets of artificial and natural drainage networks such as pipe and spring outlets),
73 may enhance microbial reduction of NO_3^- by converting it to N_2 (Schipper *et al.*,
74 2010). Bioreactor design, and in particular hydraulic retention time (HRT), is
75 therefore important to facilitate full denitrification, and can be used as a tool to
76 control indirect emissions of N_2O (Fujinuma *et al.*, 2011). These indirect emissions,
77 which may also include losses of other greenhouse gases (GHGs) such as methane
78 (CH_4) and carbon dioxide (CO_2), as well as NH_4^+ , phosphorus (P), organic C and
79 metals, is referred to as 'pollution swapping' (Fenton *et al.*, 2014). Relatively few

80 studies have considered pollution swapping in the evaluation of denitrification
81 bioreactors (Grennan *et al.*, 2009; Elgood *et al.*, 2010; Warneke *et al.*, 2011a).
82 However, no study has yet attempted to develop a metric to evaluate the performance
83 of bioreactors containing different C-rich media, which considers pollution swapping
84 across a range of HRTs, and the community of denitrifying microorganisms
85 supporting this community.

86

87 Optimal NO_3^- removal rates ($\text{g NO}_3\text{-N m}^{-3} \text{d}^{-1}$) depend on factors such as reactive
88 media type, C concentration and bioavailability (Cameron and Schipper, 2010),
89 temperature (Warneke *et al.*, 2011a); hydraulic, DO and NO_3^- loading rates (Grennan
90 *et al.*, 2009; Xu *et al.*, 2009), and HRTs (Chun *et al.*, 2009; Christianson *et al.*, 2011).
91 Typically, optimal N removal rates are determined by operating a bioreactor system
92 under various NO_3^- loading rates (Healy *et al.*, 2006). Fenton *et al.* (2009) found a
93 direct negative relationship between denitrification potential in shallow groundwater
94 and saturated hydraulic conductivity (k_s) of subsoil. Consequently, even if optimal
95 conditions for denitrification exist (Rivett *et al.*, 2008), microbially-mediated
96 reactions may be limited when k_s , or hydraulic gradients, are too high.

97

98 There has been little work on the impact of different C sources on the abundance of
99 the microbial community catalysing NO_3^- removal in denitrifying bioreactors (e.g.,
100 Moorman *et al.*, 2010; Warneke *et al.*, 2011b). Warneke *et al.* (2011b) examined this
101 by measuring the functional gene copy numbers for nitrite reductase, *nirS* and *nirK*,
102 and nitrous-oxide reductase, *nosZ*, for different C substrates, including woodchips,
103 sawdust, green waste, maize cobs and wheat straw, in laboratory bioreactors operated
104 at different temperatures (16.8 and 27.1°C). They found that microbially-mediated

105 denitrification was the main mechanism for NO_3^- -N removal, the abundance of
106 denitrifying genes was similar in all bioreactors operated at the lower temperature,
107 and that NO_3^- -N removal was mainly limited by C availability and temperature. No
108 study has yet investigated the development of denitrifying community abundance with
109 respect to distance from the inlet in a denitrifying bioreactor.

110

111 The objectives of this study were to: (1) investigate the relationship between NO_3^-
112 removal and pollution swapping during successive, incrementally decreasing HRTs
113 in denitrification bioreactors containing different C-rich media (lodgepole woodchips
114 (LPW), lodgepole pine needles (LPN), barley straw (BBS) and cardboard); (2)
115 identify optimum HRTs for each media, in which acceptable NO_3^- treatment can be
116 achieved, while minimising other losses; (3) examine whether the source of carbon in
117 a bioreactor influences the abundance of the functional genes *nirK*, *nirS* and *nosZ*.

118

119 **2. Materials and Methods**

120

121 **2.1 Operation of bioreactors**

122

123 The laboratory bioreactors of Healy *et al.* (2012) were used in the current study.
124 Briefly, these were 0.1 m-diameter x 1 m-long acrylic columns, which were loaded at
125 the base to allow even saturation and uniform flow into each column. They contained
126 either LPW, cardboard, LPN, or BBS (all at n=3), mixed in alternating 0.03 m-thick
127 layers with soil to give a C source-to-soil volume ratio of 1. Prior to operation, each
128 bioreactor was seeded with approximately 1 L of bulk fluid from a wastewater
129 treatment plant. This fluid was applied to the surface of each bioreactor and allowed

130 to percolate through the media. A control bioreactor (n=2), containing soil only
131 (CSO) was also included. The LPW and cardboard bioreactors were operated to
132 determine their long-term performance. In the Healy *et al.* (2012) study, all
133 bioreactors were loaded with NO_3^- -N solution varying from 19.5 to 32.5 mg L^{-1} at a
134 hydraulic loading rate (HLR) of 3 cm d^{-1} .

135

136 In the current study, the bioreactors were operated at incrementally increasing HLRs
137 of 5 and 10 cm d^{-1} (Table 1) and the influent NO_3^- -N concentration was varied from
138 20 to 29.6 mg L^{-1} over both loading rates. A conservative tracer (NaBr, 10 g L^{-1} ,
139 applied in one pulse in one constant hydraulic loading interval) was used to estimate
140 the average HRT within each bioreactor, at each HLR, after Levenspiel (1999).

141

142 **2.2 Water analysis**

143

144 Water samples collected at the inlet, outlet and at three sampling ports (SPs), located
145 at distances of 0.2 (SP1), 0.4 (SP2) and 0.6 m (SP3) from the inlet of each column,
146 were analysed using standard methods (APHA, 1995) for NO_3^- -N, NH_4^+ -N, nitrite-N
147 (NO_2^- -N), ortho-phosphorus (PO_4^{3-} -P), chemical oxygen demand (COD), pH and DO.
148 Nitrate removal rates (NR; g NO_3^- -N $\text{m}^{-3} \text{d}^{-1}$) were calculated taking into account the
149 Darcy velocity (q , m d^{-1}), cross sectional area (A , m^2), volume of the active area of the
150 bioreactors (m^3), and change in NO_3^- -N concentration from the inlet to outlet ($\Delta[\text{NO}_3^-$
151 $-N]$, g m^{-3}):

152

$$153 \quad NR = \frac{q \times A \times \Delta[\text{NO}_3^- - N]}{\text{media volume}} \quad (\text{g NO}_3^- \text{-N m}^{-3} \text{d}^{-1}) \quad [1]$$

154

155 **2.3 Greenhouse gas analysis**

156

157 The emission of GHG, comprising CO₂, CH₄ and N₂O, from each column was
158 measured at specific times at each HLR using the static chamber technique
159 (Hutchinson and Mosier, 1981). The headspace above each column was flushed with
160 argon (Ar) gas for 5 min at a flow rate of 3 L min⁻¹. Gas samples were withdrawn at 0,
161 15 and 30 min, and samples were analysed using a gas chromatograph (GC) (Varian
162 GC 450; The Netherlands) and automatic sampler (Combi-PAL autosampler; CTC
163 Analytics, Zwingen, Switzerland). Fluxes of CO₂, CH₄ and N₂O for each chamber
164 were measured as a function of headspace gas accumulation over time (Hutchinson
165 and Mosier, 1981). Data analyses were performed on average daily and cumulative
166 emissions by ANOVA, using the PROC GLM procedure of SAS (SAS Institute, Cary,
167 NC, 2003) with *post-hoc* least significant differences (LSD) tests used to identify
168 differences between treatments.

169

170 **2.4 Carbon, nitrogen and phosphorus analysis of soil and media**

171

172 Before construction of the bioreactors, the C and N content of all C-rich media and
173 soil were determined using a thermal conductivity detector, following combustion and
174 separation in a chromatographic column, and the P content was determined by
175 inductively coupled plasma emission spectroscopy (ICP-ES) after aqua regia
176 digestion. As the C-rich media were placed in the bioreactors in alternating 0.03 m-
177 thick layers with soil and the total mass within each reactor was measured, the initial
178 C and N content, expressed as %w/w, and the P content, expressed as mg kg⁻¹ (dry

179 matter), in each bioreactor could be calculated. Upon completion of the experiment,
180 two denitrifying bioreactors from each treatment were destructively sampled and
181 samples from four sections, each 0.2 m in length, of each bioreactor (inlet to SP1, SP1
182 to SP2, SP2 to SP3, SP3 to SP4) were analysed for C, N and P content. This enabled
183 the relationship between total C loss within each bioreactor and the cumulative COD
184 loss, the C content of the bioreactors, and the loss of P to be deduced for the period of
185 operation.

186

187 **2.5 DNA extraction and real-time PCR analysis on the media**

188

189 Real time PCR was used to quantify the archaeal and bacterial 16S rRNA populations
190 present in each bioreactor, as well as populations of denitrifying microorganisms
191 using the denitrifying genes, *nirK*, *nirS* and *nosZ* (Table 2). Archaeal and bacterial
192 16S rRNA populations were distinguished by using two sets of primers and specific
193 probes for each group. Results are described as gene copy concentrations per gram of
194 soil (GCCs/GCs g_[soil]⁻¹).

195

196 Soil used for microbiological analysis was sampled from each 0.2-m-length of each
197 column (inlet to SP1, SP1 to SP2, SP2 to SP3, SP3 to SP4), and the genomic DNA
198 was extracted from 0.5 g/ soil using the UltraClean™ Soil DNA Isolation kit
199 following the manufacturer's guidelines. The extracted genomic DNA was visualized
200 on 1% (w/v) 1X TAE agarose gels and was quantified using the Nanodrop 2000c
201 spectrophotometer (Thermo Scientific Inc). Extracted DNA was then stored at -20°C.

202

203 Standard curves for absolute quantification of archaeal and bacterial 16S rRNA genes
204 and the *nirS*, *nirK* and *nosZ* denitrification genes were constructed using the
205 corresponding standard strains and primer/probe sets outlined in Barrett *et al.* (2013;
206 Table 2). Briefly, a 10-fold dilution series of each standard plasmid solution was
207 prepared and analysed using the Light Cycler 480 (Roche, Mannheim, Germany);
208 real-time PCR was carried out in duplicate employing the corresponding primer/probe
209 set outlined in Yu *et al.* (2005) and Barrett *et al.* (2013). For the archaeal 16S rRNA
210 gene, an equimolar mixture of the corresponding standard plasmids was used as the
211 template solution for construction of the standard curve (Yu *et al.*, 2005; Lee *et al.*,
212 2009). Bacterial and archaeal 16S rRNA genes were analysed in duplicate using the
213 Light Cycler 480 (Roche, Mannheim, Germany), the LightCycler 480 Taqman
214 hydrolysis probe Master kit (Roche), and the corresponding primer/probe sets and
215 LightCycler 480 Probe Master kit (Roche; Table 2). The *nirK*, *nirS* and *nosZ* genes
216 were analysed using the corresponding primer sets with the LightCycler 480 SYBR
217 Green I Master kit (Roche), in a total volume of 20 μ l, according to the
218 manufacturer's instructions (Yu *et al.*, 2005; Barrett *et al.*, 2013). The thermal cycling
219 protocol was as outlined in Braker *et al.* (1998), Kandeler *et al.* (2006) and Henry *et*
220 *al.* (2006).

221

222 Changes in gene copy number between all samples generated from replicate
223 bioreactors and sampling ports using alternative C sources were analysed with one-
224 way ANOVA, followed by the *post-hoc* Tukey test (Graph Pad InStat V3). Individual
225 regression analysis of *nirK* and *nirS* gene copy number versus N₂O as for *nosZ* and N₂
226 were also carried out using Graph Pad InStat V3. Using Primer v6 (Primer-E,
227 Plymouth, UK), a Bray-Curtis resemblance matrix (Clarke *et al.*, 2006) was generated

228 for each bioreactor and sampling port using square root transformed mean 16S rRNA,
229 *nirS*, *nirK* and *nosZ* gene copy abundances. Using the resultant resemblance matrix,
230 the data were analyzed in a group average hierarchical cluster dendrogram.

231

232 **2.6 Sustainability Index**

233

234 Fenton *et al.* (2014) developed a simple method to quantify the effectiveness of
235 denitrification bioreactors, which considered ‘pollution swapping’. In this method, the
236 removal or production of each measured parameter is considered separately. To create
237 equivalence between water and gas measurements, all parameters are expressed in g
238 m⁻² (of bioreactor surface area) d⁻¹ and the GHGs are expressed in CO₂ equivalents to
239 account for global warming potential. Negative and positive balances of each
240 parameter indicate either removal or production of the parameter of interest. A
241 sustainability index (SI) is then created by adding each of these parameters together,
242 after Fenton *et al.* (2014):

243

$$244 \quad SI = a(B_{N_2O}) + b(B_{NO_3^-}) + c(B_{CH_4}) + d(B_{CO_2}) + etc..... \quad [2]$$

245

246 where B_x denotes the net flux (either positive or negative) of a specific parameter (x)
247 from the denitrification bioreactor, and a , b , c , etc. are weighting factors that depend
248 on the context of the analysis (e.g. legislative, environmental, geographical). For
249 example, if NO_3^- was considered the most important parameter, the weighting factor b
250 in Eqn. 2 would be set at 1 and all other parameters would be less than 1. Three
251 simple scenarios are considered in this study - Scenario 1: In countries where NO_3^-
252 removal is of most interest and GHG emissions to the atmosphere are perceived as

253 secondary, the weighting factor for NO_3^- is set to 1 and those for the other measured
254 parameters ($\text{NH}_4^+\text{-N}$, $\text{PO}_4^{3-}\text{-P}$, CH_4 , CO_2 and N_2O) are set to zero; Scenario 2: In
255 countries where legislative drivers are focused on water quality and losses of GHG to
256 the atmosphere are considered less important, appropriate weighing factors are
257 applied to NO_3^- , PO_4^{3-} and NH_4^+ ; GHGs are not considered and are set to zero. Taking
258 Ireland as an example, the maximum admissible concentration (MAC) for molybdate-
259 reactive phosphorus (MRP = $\text{PO}_4^{3-}\text{-P}$ in the current study) and NH_4^+ in rivers is $35 \mu\text{g}$
260 P L^{-1} and $65 \mu\text{g N L}^{-1}$, respectively, while NO_3^- in groundwater should not exceed
261 8.47 mg N L^{-1} (the current threshold, whereas 11.3 mg N L^{-1} is the MAC). As $\text{PO}_4^{3-}\text{-P}$
262 is the most sensitive parameter in this case, the weighting factors for $\text{PO}_4^{3-}\text{-P}$, $\text{NH}_4^+\text{-N}$
263 and $\text{NO}_3\text{-N}$ are set to 1, 0.538 (35/65) and 0.004 (35/847), respectively; Scenario 3:
264 Gaseous and water emissions are considered. Here, the weighting factor for CO_2 , CH_4
265 and N_2O is set at 1, 25 and 296, respectively, and is expressed in CO_2 equivalents
266 (IPCC, 2013). A scoring system was used across the three scenarios, with the best
267 performing media assigned the lowest score. This methodology is very much a
268 preliminary approach as to how a SI may be developed. However, it provides a
269 framework to which a more nuanced holistic analysis of the performance of a
270 bioreactor may be performed.

271

272 **3. Results**

273

274 **3.1 Removals within each media type**

275

276 The influent and effluent $\text{NO}_3^-\text{-N}$ concentrations in all bioreactors at the three HLRs
277 examined are illustrated in Figure 1. For all HLRs the N removal, expressed in terms

278 of influent and effluent NO_3^- -N concentrations (single contaminant approach) in the
279 cardboard, LPN and BBS bioreactors, were above 99.4%. The LPW and the
280 cardboard bioreactors had comparable NO_3^- -N removals to the other bioreactors
281 during the first and second HLRs, but both had average removals of 57.7 to 77.2% for
282 a HLR of 10 cm d^{-1} . The ratio of C lost from the LPW bioreactors over their total
283 period of operation (Figure 2) to the N loading on the bioreactors was, on average,
284 22:1 – higher than the optimal ratio of around 10:1 for the occurrence of
285 denitrification (Henze et al., 1997). This means that denitrification was not limited by
286 C availability (bioavailability of carbon was not measured in the current study). This
287 suggests that another process was causing the poor NO_3^- -N removal. This may have
288 been the HRT (Figure 3), as one set of LPW bioreactors with an average HRT of 3.7 d
289 (the lowest HRT measured in the study) had low NO_3^- -N removals. However, LPW
290 bioreactors performed well at a HRT of 4.9 d (Figure 3). At the end of the experiment,
291 all bioreactors were operated for 28 d at the first HLR (3 cm d^{-1}) to determine if the
292 HRT limited their performance. During this time, the bioreactors returned to almost
293 100% NO_3^- -N removal (single contaminant approach, results not shown), which
294 confirmed that bioreactors should be operated at a HRT of between 5 and 10 d for
295 optimal NO_3^- -N removal (assuming operational temperature, bioreactor construction
296 and influent concentrations are similar to this study).

297

298 The bioreactors containing LPN had a large initial release of COD (up to $5,000 \text{ mg L}^{-1}$)
299 1), which lasted for approximately 200 days of operation (Figure 4). During this
300 period, up to 80% of the total carbon at each depth increment was lost from the LPN
301 bioreactors (Figure 2). The results from all bioreactors indicate that there is a strong

302 relationship ($R^2 = 0.73$) between the % of total carbon loss and cumulative COD
303 released, according to the following equation:

304

$$305 \text{ Cumulative COD release (g)} = 5.77 \times \text{TC loss (\%)} - 3.4 \quad [3]$$

306

307 Most of the NO_3^- removal occurred within 0.4 to 0.6 m from the inlet of all
308 bioreactors (Figure 5) for all the HLRs examined. This suggests that, excluding LPW
309 bioreactors, there may have been some capacity to reduce the HRT without adversely
310 affecting system performance. This is supported by Figure 3, which indicates that,
311 with the exception of LPW bioreactors (whose performance reduced below a HRT of
312 4.9 d), NO_3^- -N removal increased with decreasing HRT. Although there was an initial
313 release of NH_4^+ -N after system start up (Figure 6), with the exception of the LPW
314 bioreactors, there was no significant release of NH_4^+ -N at any depth increment within
315 the bioreactors (Figure 7). This indicates that dissimilatory nitrate reduction to
316 ammonium (DNRA), or any other microbially-mediated process, may either have
317 only occurred at bioreactors start up when highly reducing conditions existed and
318 when there was less dilution of the released NH_4^+ -N.

319

320 Although the LPW had a P content of 41.9 mg kg^{-1} (the lowest of all the media
321 examined; Healy et al., 2012), it had the highest concentration of PO_4^{3-} -P (1.1 mg
322 PO_4^{3-} -P L^{-1}) in the final effluent (Figure 8). (Cardboard had a P content of 96.1 mg kg^{-1}
323 and also had a final effluent concentration close to 1 mg PO_4^{3-} -P L^{-1}). However, in
324 both cases, elevated P release occurred at the start of operation (at 3 cm d^{-1}). For all
325 media tested, the P content of the bioreactors did not change much from their initial P
326 content (calculated per weight of soil and media mixture; results not shown). This

327 indicates that the P was relatively immobile and, even under anaerobic conditions, P
328 was not released from the bioreactors in large amounts.

329

330 **3.2 Greenhouse gas emissions**

331

332 Mean daily GHG emissions associated with different media are shown in Figure 9.

333 Nitrous oxide emissions were generally extremely low, ranging from 0.04 – 8.8 mg

334 $\text{N}_2\text{O-N m}^{-2} \text{ d}^{-1}$. With the exception of the CSO and BBS bioreactors (where emissions

335 never rose above 0.4 mg $\text{N}_2\text{O-N m}^{-2} \text{ d}^{-1}$), the highest N_2O emissions occurred at the

336 highest loading rate (Figure 10), with fluxes of 1.48, 7.1 and 8.8 mg $\text{N}_2\text{O-N m}^{-2} \text{ d}^{-1}$ for

337 cardboard, LPW and LPN, respectively. Methane emissions ranged from 0.04 mg

338 $\text{CH}_4\text{-C m}^{-2} \text{ d}^{-1}$ in the CSO bioreactors at the 10 cm d^{-1} loading rate to 8.9 g $\text{CH}_4\text{-C m}^{-2}$

339 d^{-1} for cardboard at the 3 cm d^{-1} loading rate. Emissions from the BBS bioreactors

340 were also high at the lowest loading rate (3.0 g $\text{CH}_4\text{-C m}^{-2} \text{ d}^{-1}$). Indeed, with the

341 exception of LPW and LPN bioreactors, the highest mean daily $\text{CH}_4\text{-C}$ emission rate

342 for all media occurred at the lowest loading rate (Figure 10). A similar emissions

343 pattern is evident for CO_2 , with the highest observed flux for cardboard and BBS

344 bioreactors at the 3 cm d^{-1} loading rate (5.7 g $\text{CO}_2\text{-C m}^{-2} \text{ d}^{-1}$ and 2.25 g $\text{CO}_2\text{-C m}^{-2} \text{ d}^{-1}$,

345 respectively). The CO_2 rates for the CSO bioreactors were consistently the lowest for

346 all loading rates (Figure 10).

347

348 In terms of global warming potential (GWP), GHG fluxes were dominated by CH_4

349 emissions (Figure 9). This is because the GWP of CH_4 is 25 times higher than CO_2 ,

350 even though the fluxes were similar in terms of the mass of C released. Total GHG

351 fluxes ranged from $>0.1 \text{ g CO}_2\text{-eq m}^{-2} \text{ d}^{-1}$ for the soil control to 296 g $\text{CO}_2\text{-eq m}^{-2} \text{ d}^{-1}$

352 for CCB at the lowest loading rate (Figure 9). Emissions from CCB varied from 85 -
353 296 g CO₂-eq m⁻² d⁻¹, over 50 times higher than for all other media, with the
354 exception of BBS at the 2 cm d⁻¹ and 5 cm d⁻¹ loading rates (Figure 9).

355

356 **3.3 Microbiological results**

357

358 Using one-way ANOVA, GCCs appeared to vary significantly within the bioreactors
359 (P < 0.0001). The bacterial GCCs recorded varied significantly (P = 0.0008), with the
360 bacterial GCCs from the cardboard bioreactors considerably greater than all other
361 bioreactors (P<0.05). Archaeal GCCs varied significantly between the bioreactors and
362 sampling ports (P = 0.0049; Figure 11). The abundance of the denitrifying genes *nirS*,
363 *nirK* and *nosZ* was significantly different in all bioreactors (P = 0.0303; P = 0.0054; P
364 = 0.0043). The most abundant denitrifying gene was *nirS*, for which the highest GCCs
365 were recorded 0.2 m from the inlet of the cardboard bioreactor (1.32 x 10⁸ GCC g⁻¹
366 dry substrate). *NirS* GCCs from the cardboard bioreactors were significantly greater
367 than the CSO bioreactors (P<0.05). Overall, recorded *nirS* GCCs were greater than
368 *nirK* GCCs. The *nirK* GCCs in the cardboard bioreactors were significantly higher
369 than the CSO, LPN and LPW bioreactors (P<0.05; P<0.05; P<0.05). The *nosZ* GCCs
370 in the cardboard bioreactors were also significantly greater than the CSO, BBS and
371 LPN bioreactors (P<0.01; P<0.05; P<0.05). Using Primer v6, a Bray-Curtis
372 resemblance matrix was generated for each bioreactor and sampling port using square
373 root transformed mean 16S rRNA, *nirS*, *nirK* and *nosZ* gene copy abundances. The
374 resultant resemblance matrices from the Bray-Curtis analysis of the total and
375 denitrifying bacterial communities (from molecular data) showed that there was
376 clustering between sampling ports from each bioreactor i.e. CSO bioreactors display a

377 90-100% similarity between its sampling ports (results not shown). The LPN and
378 LPW bioreactor sampling ports were clustered together and had an 80-90% similarity,
379 whereas the CSO and cardboard bioreactors displayed a 60-70% similarity.

380

381 **4. Discussion**

382

383 **4.1 Nitrate removal**

384

385 The maximum NO_3^- -N removal rate measured was approximately $3.5 \text{ g NO}_3^- \text{-N m}^{-3} \text{ d}^{-1}$,
386 which is similar to other laboratory studies using wood-based media (e.g., 1.3 to 6.2
387 $\text{g NO}_3^- \text{-N m}^{-3} \text{ d}^{-1}$, Warneke *et al.*, 2011b; 3.9 $\text{g NO}_3^- \text{-N m}^{-3} \text{ d}^{-1}$, Grennan *et al.*, 2009;
388 3.4 $\text{g NO}_3^- \text{-N m}^{-3} \text{ d}^{-1}$, Schmidt and Clark, 2012), but much lower than some studies
389 using wood-based media (e.g., Robertson, 2010). Although the total carbon content
390 and the ratio of C lost from the bioreactors over their total period of operation to the
391 N loading on the bioreactors was adequate to sustain denitrification, the
392 bioavailability of C was not measured. Other methods may be used to assess the
393 denitrification potential of bioreactor media, such as Schmidt and Clark (2013), who
394 assessed the long-term denitrification potential of various media by calculating the
395 effluent DOC load (in g DOC m^{-3} of media per day) over time. It is unlikely that NO_3^-
396 -N removal rates were limited by the influent NO_3^- -N concentration, which was
397 between 19.5 and 32.5 mg L^{-1} , or by the slow reaction kinetics in the conversion of
398 NO_3^- to N_2 , as NO_3^- -N removals increased with reducing HRT. However, bioreactor
399 performance may have been affected by the operational temperature (10°C), as shown
400 in other studies (Cameron and Schipper, 2010; Warneke *et al.*, 2011b).

401

402 Nitrite reductase genes (*nirS* and *nirK*) ranged from 10^4 to 10^7 GCC g^{-1} dry substrate
403 in this study (Figure 11), which is in the same range measured by Warneke *et al.*
404 (2011b). As the NH_4^+ -N concentration at the outlet from all bioreactors was generally
405 low, it is unlikely that DNRA contributed significantly to NO_3^- -N removal. This
406 indicates that denitrification was most likely the main mechanism for NO_3^- -N
407 removal, the extent of which was affected by the bioreactor HRT (Figure 3). The pH
408 measured along the sampling ports and the outlet was in the optimal range for
409 denitrifiers (pH 7–8; Tchobanoglous *et al.*, 2003). The inverse relationship between
410 the HRT and NO_3^- -N removal rate, combined with the lack of a discernible trend in
411 nitrite reductase genes along the bioreactors (Figure 11), suggests that, with the
412 exception of LPW bioreactors, a shorter HRT would not have any adverse impact on
413 performance. These findings are, however, very specific to this study. In field-scale
414 bioreactors, HLR is very difficult to control, so bioreactors should be designed so that
415 they have an adequate HRT for the effective reduction of NO_3^- .

416

417 **4.2 Denitrifying bacterial communities**

418

419 The CCB bioreactors had the greatest average abundance of denitrification genes but
420 lowest number of denitrification genes as a proportion of total bacteria and the highest
421 number of 16S rRNA GCC g^{-1} . Excluding the control bioreactors, the other
422 bioreactors (BBS, LPN and LPW) had a similar number of denitrification genes and
423 total bacterial DNA, and both parameters were at least an order of magnitude less than
424 the cardboard bioreactors. The LPN and LPW bioreactors had the highest number of
425 denitrification genes as a proportion of total bacteria. This implies that a greater
426 proportion of C in cardboard bioreactors was consumed by non-denitrifying bacteria,

427 fungi or yeasts, whereas a greater proportion of C in the LPN and LPW bioreactors
428 was consumed by denitrifiers. In order to verify this, further work would be necessary
429 targeting alternative stains. The fact that a greater proportion of denitrifiers were
430 present in the LPN/LPW media coincided with higher N₂O emissions, which were
431 observed in both media at the highest loading rate. This increase in N₂O level also
432 coincided with a decrease in the efficiency of NO₃⁻ removal at the highest loading
433 rate. It may indicate either partial denitrification to N₂O *in situ* or degassing of
434 dissolved N₂O in the original water in the column.

435

436 The ratio of *nirS/nirK* and total number of nitrite reductase genes (Σnir)/*nosZ* was
437 similar between replicate bioreactors and within each 0.2-m-depth in every bioreactor.
438 There was no indication that populations of denitrifying or non-denitrifying bacteria
439 were grouped at any particular point within the bioreactors (i.e. towards the inlet or
440 outlet). The nutrient concentrations measured at each 0.2-m-depth increment were
441 consistent with this finding (Figures 5 and 7). There appears to be a greater variation
442 in denitrifying gene number and presence between the reactors than within an
443 individual reactor, based on the sampling resolution used. Indicating microbial
444 populations and activity established in each bioreactor therefore reflect and respond to
445 the nature of the media therein (and microbial evolution of the system), as opposed to
446 operation of the bioreactor (i.e. HRT). Overall, this suggests that gene analysis may
447 be employed to reliably assess the relative dominance of the denitrifying microbial
448 populations. Further work is necessary to determine if it could be used as a potential
449 proxy for bioreactor design and optimisation.

450

451 **4.3 Greenhouse gases**

452

453 Anoxic to anaerobic conditions in the bioreactors resulted in high levels of CH₄ efflux
454 and relatively low CO₂ and N₂O loss. Anaerobic conditions result in the complete
455 denitrification of nitrite and subsequently nitrate to N₂. As a result, the N₂O flux in the
456 bioreactors was very low and negative fluxes were observed in some cases; in these
457 instances, *nir* GCCs were lower than *nosZ* GCCs. A significant flux was only
458 observed at higher HLRs, where the presence of dissolved O₂ in the influent may
459 allow some partial denitrification to N₂O. This, combined with the higher pressures in
460 the system, may subsequently result in the degassing of dissolved N₂O, and coincided
461 with decreased nitrate removal from the bioreactors.

462

463 Apart from the cardboard medium, CO₂ release from heterotrophic respiration was
464 very low compared with normal rates of (7- 30 g CO₂ m⁻² d⁻¹) of soil respiration
465 (Lloyd and Taylor, 1994). The higher rate of CO₂ and CH₄ efflux in the cardboard
466 bioreactors reflected the successional mobilisation of organic C *via* heterotrophic and
467 anaerobic respiration, and was also related to the archaeal 16SrRNA GCC abundance.
468 Carbon within the media was utilised principally by denitrifying bacteria, generating
469 CO₂ that was either directly emitted or consumed by methanogens as the terminal
470 electron acceptor in methanogenesis (Wolin and Miller, 1987). The lower rates
471 observed in LPW, LPN and CSO bioreactors (0.02 mg CH₄ m⁻² d⁻¹ to 0.34 mg CH₄ m⁻²
472 d⁻¹ for soil and LPW bioreactors, respectively) were comparable to typical values of
473 diffusional (non-ebullition) methane fluxes from peatlands, which range from 1.5–480
474 mg CH₄ m⁻² d⁻¹ (Coulthard *et al.*, 2009). The higher rates in the cardboard (8.8 mg
475 CH₄ m⁻² d⁻¹) and, to a lesser extent, BBS bioreactors (3 mg CH₄ m⁻² d⁻¹), reflect higher
476 rates of microbial activity presumably due to more labile C sources. Emissions from

477 both these media were greatest at the lowest loading rates (2.5 to 8.8 g CH₄-C m⁻² d⁻¹),
478 equating to an annual methane loss of between 1.3 and 4.3 kg CH₄ m⁻² yr⁻¹. These
479 emissions are similar to localised methane ebullition from peatlands, where fluxes can
480 range from 1.2 to 26 g CH₄-C m⁻² d⁻¹ (Glazer *et al.*, 2004; Tokida *et al.*, 2007).

481

482 The high total GHG emissions from CCB and BBS bioreactors were dominated by
483 methane and were 50 times higher than other media, which had comparable or better
484 nitrate removal. As such, these media should be avoided in bioreactors or if they are
485 used, some form of remedial action, such as soil capping, should be utilised to oxidise
486 some of the methane and reduce this flux to the atmosphere (Stern *et al.*, 2007).

487

488 **4.4 Identification of optimum loading rates considering pollution swapping**

489

490 The net flux of each parameter of interest in this study is shown in Table 3 and the SI
491 calculations for three scenarios (1=only NO₃⁻ considered; 2=all mixed contaminants
492 in water; and 3=water and gaseous emissions) are presented in Table 4. For Scenario
493 1, LPW bioreactors performed best at the lowest HLR, and cardboard and LPN
494 bioreactors performed best at the two higher HLRs. In Scenario 2, BBS bioreactors
495 had the best performance across all HLRs. In Scenario 3, LPN bioreactors performed
496 best at HLRs of 3 and 5 cm d⁻¹, whereas LPW bioreactors performed best at a HLR of
497 10 cm d⁻¹. Considering all water quality and gaseous parameters for the three
498 scenarios, analysed at each HLR, the LPN bioreactors performed best. However, there
499 was an 80% reduction in TC from the LPN bioreactors over its operation period
500 (approximately 560 days) (Figure 2). In comparison, the LPW bioreactors only

501 experienced a TC loss of approximately 27% over 745 days of operation, which
502 suggests this type of bioreactor may have greater longevity than LPN bioreactors.

503

504 It is important for research to start moving from single contaminant to mixed
505 contaminant mitigation, as conceptualised by Fenton *et al.* (2014). The type of
506 analysis conducted in this study is considerably simplified, but highlights the huge
507 disadvantages of the single contaminant approach. In reality, attributing weighting
508 factors to both dissolved contaminants and GHGs would be considerably more
509 complex, and require consideration of their respective costs and benefits, local
510 legislation and environmental conditions, as well as cognisance of the fact that
511 legislation will change over time. If total removal of mixed contaminants, apart from
512 achievement of maximum admissible concentrations or targets, is the goal, more
513 efficient systems will need to be envisaged for the future. The co-location of
514 denitrifying bioreactor and adsorption structures in sequence – termed “permeable
515 reactive interceptors” – is a move in this direction (Fenton *et al.*, 2014).

516

517 **5. Conclusions**

518

519 The way in which the performance of denitrifying bioreactors is assessed can lead to
520 different conclusions about optimum HRT and media selection. When NO_3^- removal
521 only was assessed (single contaminant approach), there was a net removal in all
522 bioreactors, which increased as HRT reduced. All bioreactors performed best at HRTs
523 of around 5 days. When all contaminants (NO_3^- , NH_4^+ and PO_4^{3-}) were considered,
524 there was a net flux of contaminants from all columns, which further increased when
525 greenhouse gas emissions were also considered. To reduce pollution swapping from

526 bioreactors, suitable media could be placed in sequence in the filters, which would be
527 capable of reducing the contaminant of interest before final discharge. Based on the
528 study results, LPN bioreactors appeared to be the most effective design, across all
529 HRTs and scenarios, at effectively treating NO_3^- , while limiting pollution swapping.
530 However, a substantial amount of carbon was lost over a relatively short period
531 (around 80% of the initial content of the LPN bioreactors). This indicates that a more
532 commonly available filter media, such as LPW, may be more suitable for the long-
533 term operation of bioreactors.

534

535 Microbiological testing of the filter media at the end of the experiment indicated that
536 denitrification was most likely the main mechanism for NO_3^- -N removal and that
537 there was no clustering of the denitrifying or non-denitrifying bacteria at any
538 particular point within the bioreactors. The addition of carbon appeared to affect the
539 abundance of denitrifiers possessing the targeted functional genes. Moreover, the
540 cardboard bioreactor contained the highest abundance of denitrifying microorganisms
541 compared with the other bioreactors, indicating that the source of carbon influenced
542 the abundance of denitrifying microbes. Microbiological analyses, such as those
543 performed in this study, could be used as a proxy for system performance at various
544 HRTs with further testing. However, this analysis could not be performed in the
545 current study, as the microbiological testing was conducted in the columns having
546 been subjected to three HLRs.

547

548 **Acknowledgements**

549

550 This study was funded under the Department of Agriculture, Fisheries and Food under
551 the Research Stimulus Programme 2007 (RSF 07 525).

552

553

554

555

556

557

558

559

560

561

562

563

564

565

566

567

568

569

570

571

572

573

574

575 **References**

576

577 APHA, 1995. Standard methods for examination of water and wastewater, 19th ed.

578 American Public Health Association, Washington, DC.

579

580 Barrett, M., Jahangir, M.M.R., Lee, C., Smith, C.J., Bhreathnach, N., Collins, G.,

581 Richards, K.G., O’Flaherty, V., 2013. Abundance of denitrification genes under

582 different piezometer depths in four agricultural groundwater sites. *Environmental*

583 *Science and Pollution Research* 20 (9), 6646-6657.

584

585 Braker, G., Fesefeldt, A., Witzel K.P., 1998. Development of PCR primer systems for

586 amplification of nitrite reductase genes (*nirK* and *nirS*) to detect denitrifying bacteria

587 in environmental samples. *Applied and Environmental Microbiology* 64 (10), 3769-

588 3775.

589

590 Cameron, S.G., Schipper, L.A., 2010. Nitrate removal and hydraulic performance of

591 organic carbon for use in denitrification beds. *Ecological Engineering* 36 (11), 1588 –

592 1595.

593

594 Christianson, L.E., Bhandari, A., Helmers, M.J., 2011. Pilot-scale evaluation of

595 denitrification drainage bioreactors: reactor geometry and performance. *ASCE*

596 *Journal of Environmental Engineering* 137 (4), 213 – 220.

597

598 Chun, J.A., Cooke, R.A., Eheart, J.W., Kang, M.S., 2009. Estimation of flow and

599 transport parameters for woodchip-based bioreactors: I. laboratory-scale bioreactor.

600 *Biosystems Engineering* 104 (3), 384 – 395.

601

602 Clarke, K.R, Somerfield, P.J., Chapman, M.G., 2006. On resemblance measures for

603 ecological studies, including taxonomic dissimilarities and a zero-adjusted Bray–

604 Curtis coefficient for denuded assemblages. *Journal of Experimental Marine Biology*

605 *and Ecology* 330 (1), 55–80.

606

607 Coulthard, T.J., Baird, A. J., Ramirez, J., Waddington J. M., 2009. Methane dynamics

608 in peat: importance of shallow peats and a novel reduced-complexity

609 approach for modeling ebullition. In: A.J. Baird, L.R. Belyea, X. Comas, A. S. Reeve,

610 and L. D. Slater (Eds.) *Carbon Cycling in Northern Peatlands*. American Geophysical

611 Union, Washington.

612

613 Durand, P., Breuer, L., Johnes, P.J., 2011. Nitrogen processes in aquatic ecosystems.

614 Pp. 126-146. In: M.A. Sutton, C.M. Howard, J.W. Erisman, G. Billen, A. Bleeker, P.

615 Grennfelt, H. van Grinsven, B. Grizzetti (eds.), *The European Nitrogen Assessment-*

616 *Sources, Effects and Policy Perspectives*. Cambridge University Press, Cambridge.

617

618 Elgood, Z., Robertson, W.D., Schiff, S.L., Elgood, R., 2010. Nitrate removal and

619 greenhouse gas production in a stream-bed denitrifying bioreactor. *Ecological*

620 *Engineering* 36 (11), 1575 – 1580.

621

622 Fenton, O., Richards, K.G., Kirwan, L., Healy, M.G., 2009. Factors affecting nitrate

623 distribution in shallow groundwater using a beef farm in south eastern Ireland. *Journal*

624 *of Environmental Management* 90 (10), 3135 – 3146.

625
626 Fenton, O., Schulte, R.P.O., Jordan, P., Lalor, S., Richards, K.G., 2011. Time lag: a
627 methodology for the estimation of vertical and horizontal travel and flushing
628 timescales to nitrate threshold concentrations in Irish aquifers. *Environmental Science*
629 *and Policy* 14 (4), 419-431.
630
631 Fenton, O., Healy, M.G., Brennan, F., Jahangir, M.M.R., Lanigan, G.J., Richards,
632 K.G., Thornton, S.F., Ibrahim, T.G., 2014. Permeable reactive interceptors – blocking
633 diffuse nutrient greenhouse gases losses in key areas of the farming landscape.
634 *Journal of Agricultural Science*. In press. doi:10.1017/S0021859613000944
635
636 Flechard C.R., Nemitz E., Smith R.I., Fowler D., Vermeulen A.T., Bleeker A., Erisman
637 J.W., Simpson D., Zhang L., Tang Y.S., and Sutton M.A., 2011. Dry deposition of
638 reactive nitrogen to European ecosystems: a comparison of inferential models across the
639 NitroEurope network. *Atmospheric Chemistry and Physics* 11 (6), 2703–2728.
640
641 Fujinuma, R., Venterea, R.T., Ranaivoson, A., Moncrief, J., Dittrich, M. 2011. On-
642 site wood-chip bioreactors could reduce indirect nitrous oxide emissions from tile
643 drain waters. In: *Proceedings of Nutrient Efficiency and Management Conference*.
644 MN Department of Agriculture, Minnesota, February 2011.
645
646 Glaser, P.H., Chanton, J.P., Morin, P., Rosenberry, D.O., Siegel, D.I., Ruud, O.,
647 Chasar, L.I., Reeve, A.S., 2004. Surface deformations as indicators of deep ebullition
648 fluxes in a large northern peatland, *Global Biogeochemical Cycles* 18 (1), 1 – 15.
649
650 Grennan, C.M., Moorman, T.B., Parkin, T.B., Kaspar, T.C., Jaynes, D.B., 2009.
651 Denitrification in wood chip bioreactors at different water flows. *Journal of*
652 *Environmental Quality* 38 (4), 1664 – 1671.
653
654 Grizzetti, B., Bouraoui, F., Aloe, A., 2012. Changes in nitrogen and phosphorus loads
655 to European seas. *Global Change Biology* 18 (2), 769-782.
656
657 Healy, M.G., Rodgers, M., Mulqueen, J., 2006. Denitrification of a nitrate-rich
658 synthetic wastewater using various wood-based media materials. *Journal of*
659 *Environmental Science and Health, Part A* 41 (5), 779 – 788.
660
661 Healy, M.G., Ibrahim, T.G., Lanigan, G.J., Serrenho, A.J., Fenton, O., 2012. Nitrate
662 removal rate, efficiency and pollution swapping potential of different organic carbon
663 media in laboratory denitrification bioreactors. *Ecological Engineering* 40 (March
664 2012), 198 – 209.
665
666 Henry, S., Bru, D., Stes, B., Hallet, S., Philippot, L., 2006. Quantitative detection of
667 the *nosZ* gene, encoding nitrous oxiden reductase, and comparison of the abundances
668 of 16S rRNA, *narG*, *nirK*, and *nosZ* genes in soils. *Applied and Environmental*
669 *Microbiology* 72 (8), 5181–5189.
670
671 Henze, M., Harremoës, P., Jansen, J.L.C., Arvin, E., 1997. *Wastewater treatment:*
672 *biological and chemical processes*. Springer, Berlin.
673

674 Hutchinson, G.L., Mosier, A.R., 1981. Improved soil cover method for field
675 measurement of nitrous oxide fluxes. *Soil Science Society of America Journal* 45 (2),
676 311 – 316.
677
678 IPCC, 2013. *Climate change 2013: The physical science basis. Contribution of*
679 *Working Group I to the fifth assessment report of the intergovernmental panel on*
680 *climate change, Ch.8, p. 714.*
681
682
683 Kandeler, E., Deiglmayr, K., Tscherko, D., Bru, D., Philippot, L., 2006. Abundance of
684 *narG*, *nirS*, *nirK*, and *nosZ* Genes of denitrifying bacteria during primary successions
685 of a glacier foreland. *Applied and Environmental Microbiology* 72 (9), 5957–5962.
686
687 Lee, C., Kima, J., Hwang, K., O’Flaherty, V., Hwang, S., 2009. Quantitative
688 analysis of methanogenic community dynamics in three anaerobic batch digesters
689 treating different wastewaters. *Water Research* 43 (1), 157-165.
690
691 Levenspiel, O. 1999. *Chemical reaction engineering.* John Wiley and Sons, New
692 York.
693
694 Lloyd J., Taylor J.A., 1994. On the temperature dependence of soil respiration.
695 *Functional Ecology* 8, 315-323.
696
697 Moorman, T.B., Parkin, T.B., Kaspar, T.C., Jaynes, D.B., 2010. Denitrification
698 activity, wood loss, and N₂O emissions over 9 years from a wood chip bioreactor.
699 *Ecological Engineering* 36 (11), 1567 – 1574.
700
701 Richardson, D., Felgate, H., Watmough, N., Thomson, A., Baggs, E., 2009.
702 Mitigating release of the potent greenhouse gas N₂O from the nitrogen cycle – could
703 enzymic regulation hold the key? *Trends in Biotechnology* 27 (7), 388 – 397.
704
705 Rivett, M.O., Buss, S.R., Morgan, P., Smith, J.W., Bemment, C.D., 2008. Nitrate
706 attenuation in groundwater: a review of biogeochemical controlling processes. *Water*
707 *Research* 42 (16), 4215 – 4232.
708
709 Robertson, W.D., 2010. Nitrate removal rates in woodchip media of varying age.
710 *Ecological Engineering* 36 (11), 1581 – 1587.
711
712 Schipper, L.A., Robertson, W.D., Gold, A.J., Jaynes, D.B., Cameron, S.C., 2010.
713 Denitrifying bioreactors – an approach to reducing nitrate loads to receiving waters.
714 *Ecological Engineering* 36 (11), 1532-1543.
715
716 Schmidt, C.A., Clark, M.W., 2012. Efficacy of a denitrification wall to treat
717 continuously high nitrate loads. *Ecological Engineering* 42 (May 2012), 203 – 211.
718
719 Stern, J.C., Chanton, J., Abichou, T., Powelson, D., Yuan, L., Escoriza, S., Bogner, J.,
720 2007. Use of a biologically active cover to reduce landfill methane emissions and
721 enhance methane oxidation. *Waste Management* 27 (9), 1248-1258.
722

723 Tchobanoglous, G., Burton, F.L., Stensel, H.D., 2003. Wastewater engineering,
724 Treatment and Reuse. McGraw Hill, New York, NY.
725
726 Tokida, T., Miyazaki, T., Mizoguchi, M., Nagata, O., Takakai, F., Kagemoto, A.,
727 Hatano, R., 2007. Falling atmospheric pressure as a trigger for methane ebullition
728 from a peatland, Global BiogeochemicalCycles 21, GB2003
729
730 Yu, Y., Lee, C., Kim, J., Hwang, S., 2005. Group-specific primer and probe sets to
731 detect methanogenic communities using quantitative real-time polymerase chain
732 reaction. Biotechnology and Bioengineering 89 (6), 670–679.
733
734 Warneke, S., Schipper, L.A., Bruesewitz, D.A., McDonald, I., Cameron, S., 2011a.
735 Rates, controls and potential adverse effects of nitrate removal in a denitrification bed.
736 Ecological Engineering 37 (3), 511-522.
737
738 Warneke, S., Schipper, L.A., Matiasek, M.G., Scow, K.M., Cameron, S., Bruesewitz,
739 D.A., McDonald, I.R., 2011b. Nitrate removal, communities of denitrifiers and
740 adverse effects in different carbon substrates for use in denitrification beds. Water
741 Research 45 (17), 5463 – 5475.
742
743 Wolin, M.J., Miller, T.L., 1987. Bioconversion of organic carbon to CH₄ and CO₂.
744 Geomicrobiology 5 (3-4), 239-59.
745
746 Xu, Z., Shao, L., Yin, H., Chu, H., Yao, Y., 2009. Biological dentrification using
747 corncobs as a carbon source and biofilm carrier. Water Environment Research 81 (3),
748 242 247.
749
750
751
752
753
754
755
756
757

758

759

760
761
762

763 **Table 1.** Media used in denitrification bioreactors, period of operation (d), hydraulic retention time (HRT; d), nitrate (NO₃⁻-N) removal
 764 (expressed as difference between inlet and outlet concentration; %) at each hydraulic loading rate (3, 5 and 10 cm d⁻¹) applied to the bioreactors.
 765

Media ^a	Column	HLR (cm d ⁻¹)			HLR (cm d ⁻¹)			HLR (cm d ⁻¹) ^b		
		3	5	10	3	5	10	3	5	10
		Period of operation (d)			HRT (d)			NO ₃ -N removal		
LPW	1	460	238	47	17.4	7.7	4.9	99.6	82.6	58.8
	2				13.0	8.1	3.7	99.6	93.1	57.7
	3				14.8	9.2	5.7	99.7	99.4	77.2
Cardboard	1	438	237	47	10.2	6.7	4.0	99.7	99.5	99.7
	2				8.5	7.4	4.8	99.5	99.4	99.7
	3				10.9	6.9	3.5	99.8	99.4	99.7
LPN	1	278	237	47	9.9	9.6	4	99.8	99.4	99.7
	2				11.6	6.7	4	99.7	99.2	99.7
	3				9.9	9.5	3.6	99.9	99.4	99.7
BBS	1	231	133	47	13.9	7.0	3.5	-	99.4	99.7
	2				21.7	8.8	3.9	-	99.7	99.7
	3				18.2	7.3	3.6	-	99.5	99.7
Soil	1	257	134	47	15.5	6.1	4.6	16.5	4.6	-1.4
	2				11.8	6.4	3.8	28.0	0.9	-0.4

766 ^a LPW = lodgepole pine woodchips; LPN = lodgepole pine needles; BBS = barley straw

767 ^b Nitrate removal and efficiency reported at steady-state only. Steady-state was not attained at a HLR of 3 cm d⁻¹ for BBS (Healy et al., 2012).

768
 769
 770
 771
 772
 773
 774

775 **Table 2** Realtime primer and probes for microbial analysis (adapted from Barrett et al., 2013)

Gene	Standard strains	Oligoneucleotide ^c	Sequences (5' – 3')	Amplicon size (bp)	Reference
<i>nirS</i>	<i>Pseudomonas Stutzeri</i> ATCC 14405 ^a	F: <i>nir</i> SCd3aF R: <i>nir</i> SR3cd	AACGYSAAGGARACSGG GASTTCGGRTGSGTCTTSAYGAA	425	Kandeler et al. (2006)
<i>nirK</i>	<i>Alcalignes</i> Species DSMZ 30128 ^b	F: <i>nir</i> k 1F R: <i>nir</i> k 5R	GG(A/C) ATG GT (G/T) CC(C/G) TGG CA GCC TCG ATC AG (A/G) TT(A/G) TGG	514	Braker et al. (1998)
<i>nosZ</i>	<i>Bradyrhizobium</i> <i>Japonicum</i> USDA 110 ^c	F: <i>nosz</i> 2 F R: <i>nosz</i> 2 R	CG(C/T)TGTT(C/A/C)TCGACAGCCAG CAKRTGCAKSGCRTGGCAGAA	267	Henry et al. (2006)
Bacterial 16SrRNA	<i>Escherichia coli</i> K12 ^d	F: BAC 338F R: BAC 805R P: BAC516F	ACTCCTACGG GAGGCAG GACTACCAGGGTATCTAATCC TGC CAG CAG CCG CGG TAA TAC	466	Yu et al. (2005)
Archaeal 16SrRNA		F:ARC787 R:ARC1059 P:ARC915	ATTAG ATACC CSBGT AGTCC AGGAA TTGGC GGGGG AGCAC GCCAT GCACC WCCTC T	273	Yu et al. (2005)

776 ^a ATCC, American type culture collection ^b DSMZ, The German Resource Centre for Biological Material ^c USDA, United States Department of Agriculture ^d Gift ^e P, TaqMan probe; F,
777 Forward primer; R, Reverse primer
778

779

780

781

782

783

784

785

786

787 **Table 3.** Net fluxes (in $\text{g m}^{-2} \text{d}^{-1}$) \pm standard deviations (in brackets) of major dissolved compounds and greenhouse gases (expressed as CO_2 equivalents per unit surface area
788 per day.) from laboratory scale denitrifying bioreactors, operated at steady-state, for the three hydraulic loading rates (HLRs), 3, 5 and 10 cm d^{-1} . Negative and positive fluxes
789 indicate remediation and production of the compound, respectively.

HLR (cm d^{-1})	Media ^a	$\text{NO}_3^- \text{-N}$	$\text{NH}_4^+ \text{-N}$	$\text{PO}_4^{3-} \text{-P}$	CH_4	CO_2	N_2O
3	LPW	-0.81 (0)	0.11 (0.01)	0.003 (0)	4.01 (2.04)	3.86 (1.04)	0.57 (0.39)
	Cardboard	-0.60 (0)	0.05 (0.01)	0.001 (0)	296.03 (26.67)	21.04 (4.41)	0.04 (0.03)
	LPN	-0.78 (0)	0.05 (0.02)	0.000 (0)	2.52 (1.26)	5.13 (1.85)	0.10 (0.04)
	BBS	-0.75 (0)	0.03 (0.01)	0.001 (0)	100.29 (55.69)	8.26 (1.35)	0.22 (0.08)
5	LPW	-1.00 (0.1)	0.03 (0)	0.018 (0.013)	11.57 (2.29)	1.51 (0.37)	1.48 (1.09)
	Cardboard	-1.09 (0)	0.03 (0.02)	0.001 (0)	99.43 (35.48)	6.88 (3.73)	0.02 (0.04)
	LPN	-1.08 (0)	0.03 (0)	0.002 (0)	0.70 (0.55)	1.38 (0.57)	0.09 (0.70)
	BBS	-1.08 (0)	0.02 (0)	0.001 (0)	38.04 (18.57)	3.10 (0.50)	0.13 (0.09)
10	LPW	-1.46 (0.24)	0.07 (0.03)	0.003 (0.001)	0 (0.01)	1.47 (0.34)	3.29 (2.88)
	Cardboard	-2.15 (0)	0.05 (0.03)	0.002 (0)	85.36 (23.19)	6.12 (2.33)	0.69 (0.78)
	LPN	-2.19 (0)	0.06 (0.01)	0.003 (0.002)	3.71 (1.47)	1.66 (0.65)	4.11 (3.28)
	BBS	-2.12 (0)	0.03 (0)	0 (0)	4.28 (1.84)	1.42 (0.69)	0.02 (0.12)

790 ^a LPW = lodgepole pine woodchips; LPN = lodgewood pine needles; BBS = barley straw

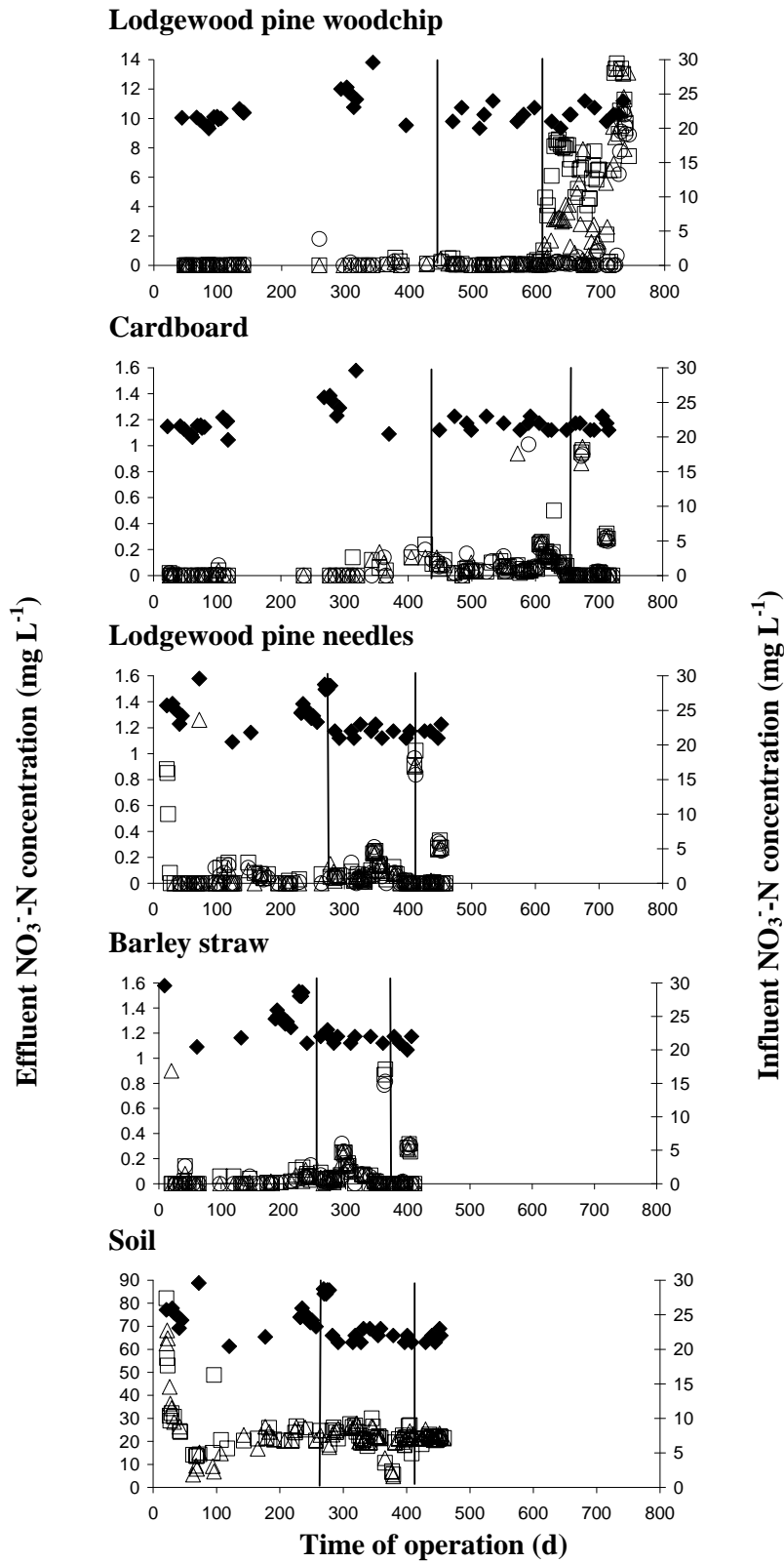
791 **Table 4.** Net flux ($\text{g m}^{-2} \text{d}^{-1}$) and sustainability index (SI) calculations, calculated
 792 from Table 3, for the filter media for three scenarios (see text for explanation).
 793 Negative and positive net fluxes indicate removal and production of the compound,
 794 respectively. A high SI indicates poor performance, a low SI indicates good
 795 performance.
 796

HLR	Media ^a	Scenario 1		Scenario 2		Scenario 3		Overall ranking ^b
(cm d^{-1})		Net flux ($\text{g m}^{-2} \text{d}^{-1}$)	SI	Net flux ($\text{g m}^{-2} \text{d}^{-1}$)	SI	Net flux ($\text{g m}^{-2} \text{d}^{-1}$)	SI	
3	LPW	-0.81	1	0.06	3	7.74	2	7
	Cardboard	-0.60	4	0.03	4	316.56	4	11
	LPN	-0.78	2	0.02	1	7.02	1	5
	BBS	-0.75	3	0.01	2	108.05	3	7
5	LPW	-1.00	3	0.03	3	13.61	2	7
	Cardboard	-1.09	1	0.01	1	105.27	4	6
	LPN	-1.08	2	0.01	2	1.12	1	4
	BBS	-1.08	2	0.01	1	40.21	3	6
10	LPW	-1.46	4	0.03	4	3.37	1	8
	Cardboard	-2.15	2	0.02	2	90.07	4	8
	LPN	-2.19	1	0.03	1	7.35	3	7
	BBS	-2.12	3	0.01	3	3.63	2	6

797 ^a LPW = lodgewood pine woodchips; LPN = lodgewood pine needles; BBS = barley straw

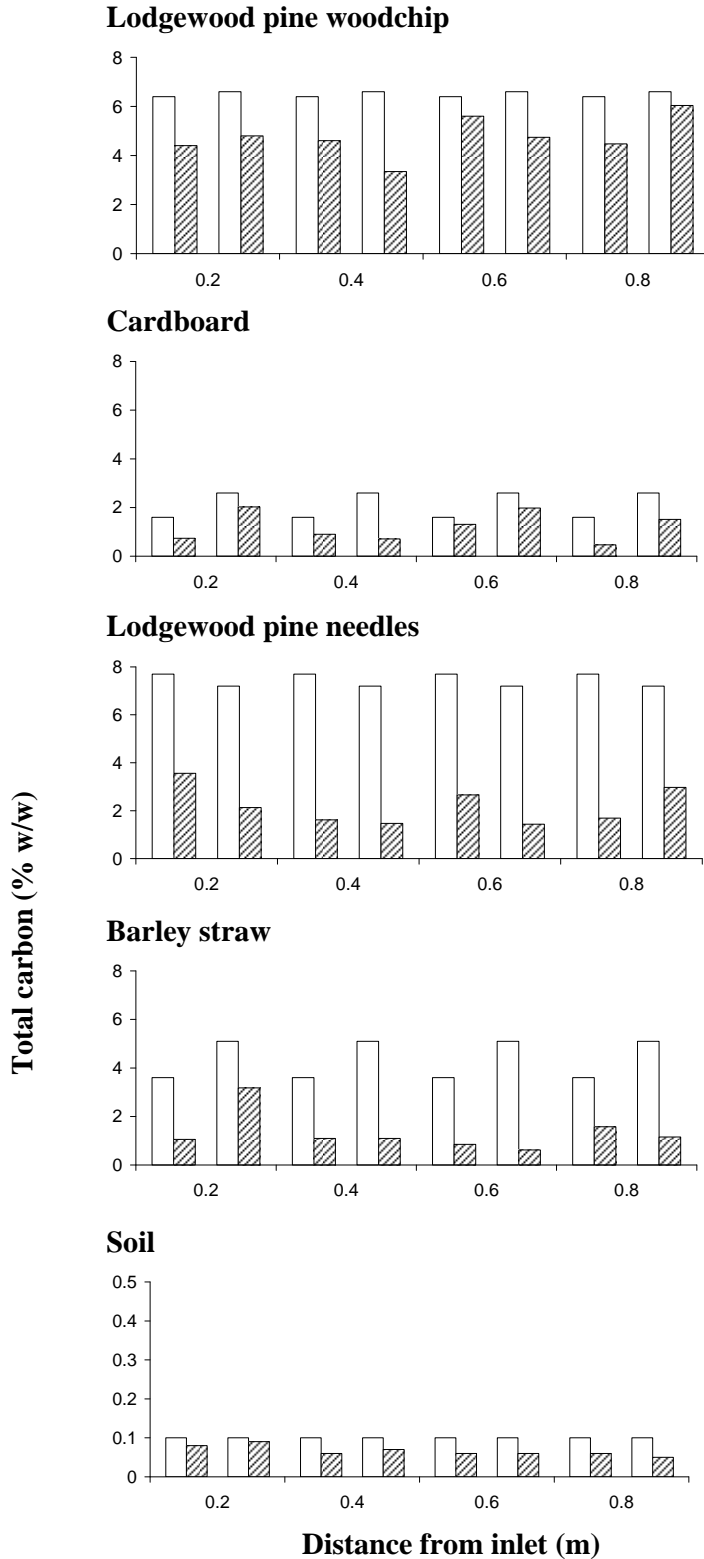
798 ^b Obtained from the sum of the sustainability indices (SIs) for each scenario

799
800
801
802
803
804
805
806
807
808
809
810
811
812
813
814
815

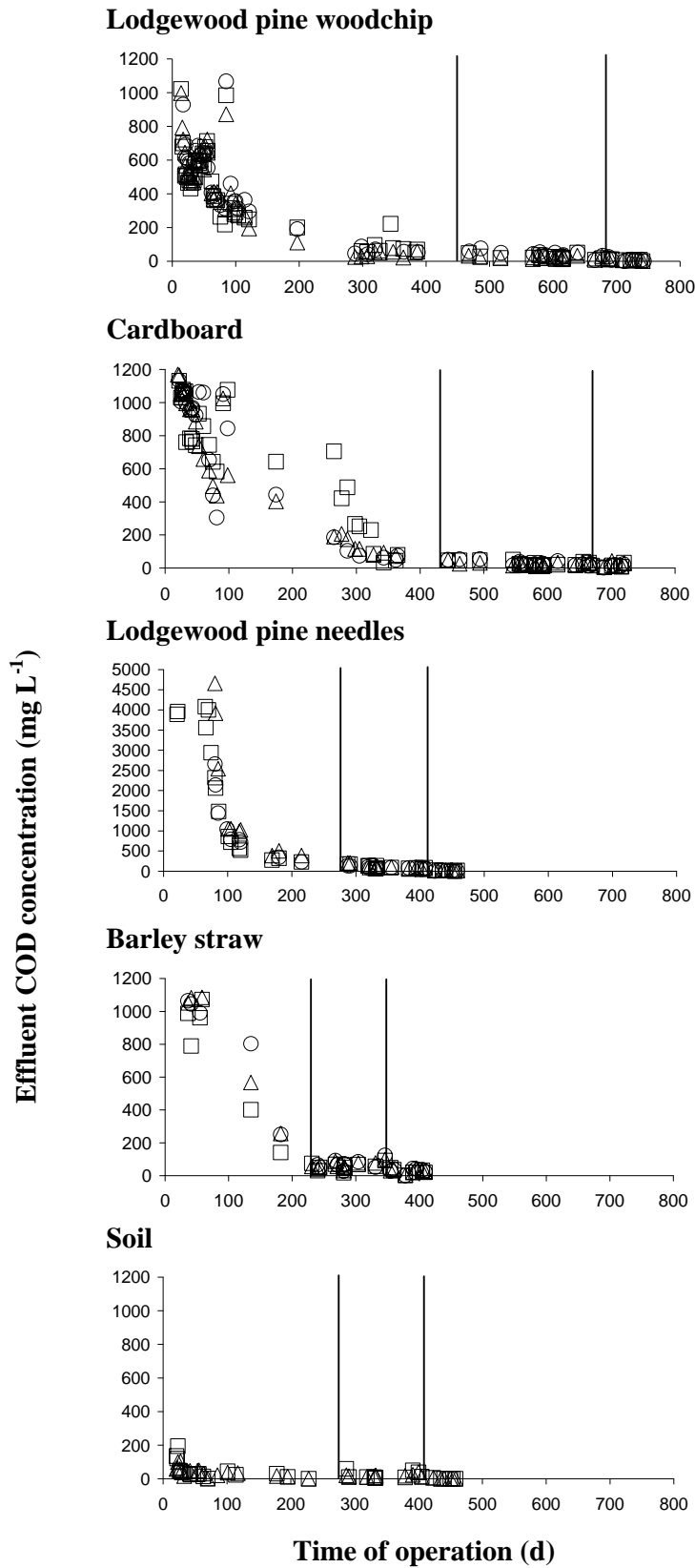


816
817
818
819
820

Figure 1. Influent and effluent nitrate concentrations and operation boundaries for each media. Open square = Column 1 effluent; Open triangle = Column 2 effluent; Open circle = Column 3 effluent; Closed diamond = influent NO_3^- -N concentration. Vertical lines represent the three hydraulic loading rates: 3, 5 and 10 cm d^{-1}

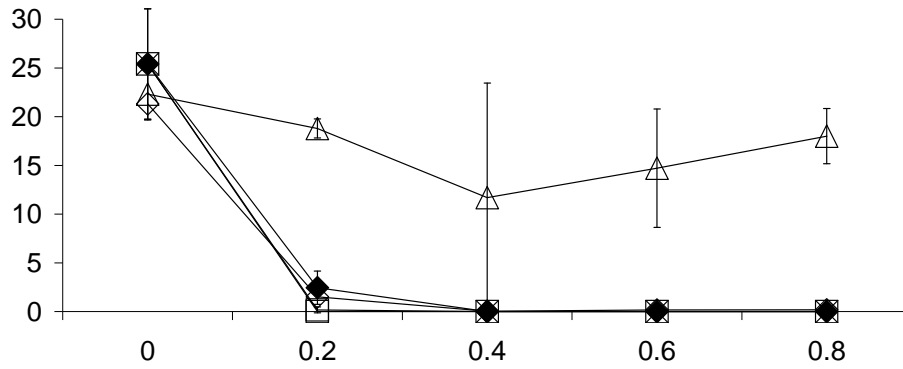


822 Figure 2. Total carbon, expressed as a % of total carbon per dry weight of material
 823 (soil + filter media) in each 0.2 m depth of the bioreactors (n=2) at the start and end of
 824 the study. White boxes = total carbon (%w/w) at the start of the study. Hatched boxes
 825 = total carbon (%w/w) at the end of the study.

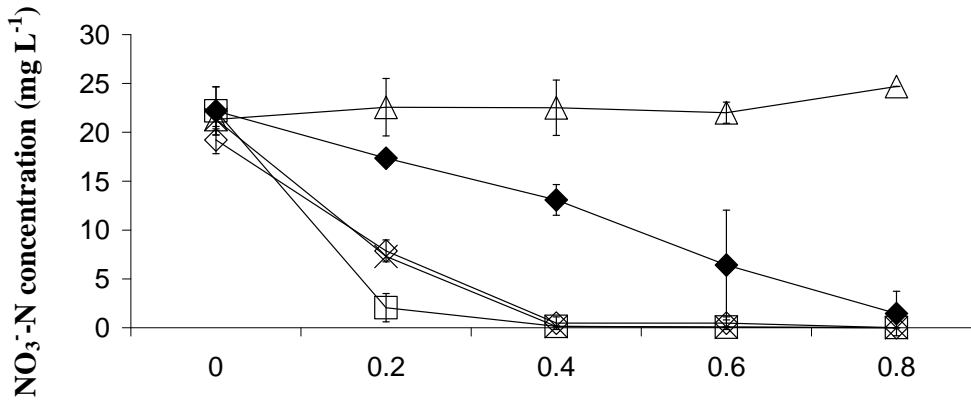


859 Figure 4. Effluent COD concentrations and operation boundaries for each media. Open square =
 860 Column 1; Open triangle = Column 2; Open circle = Column 3. Vertical lines represent the three
 861 hydraulic loading rates: 3, 5 and 10 cm d⁻¹.

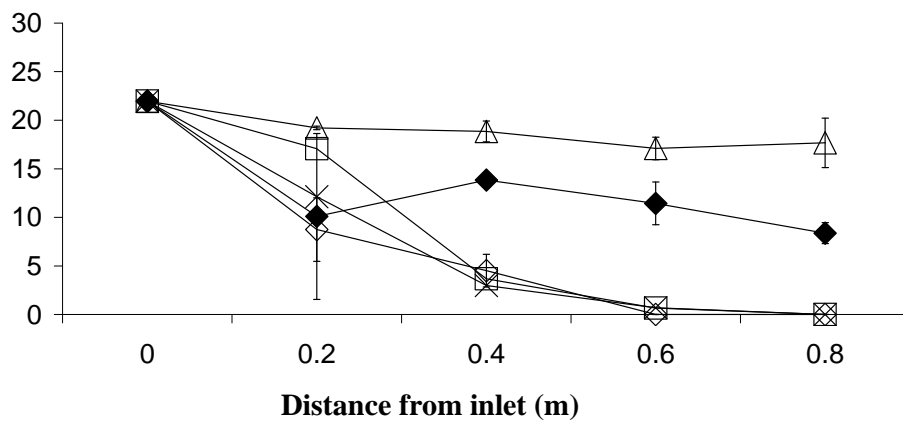
Hydraulic loading rate: 3 cm d⁻¹



Hydraulic loading rate: 5 cm d⁻¹



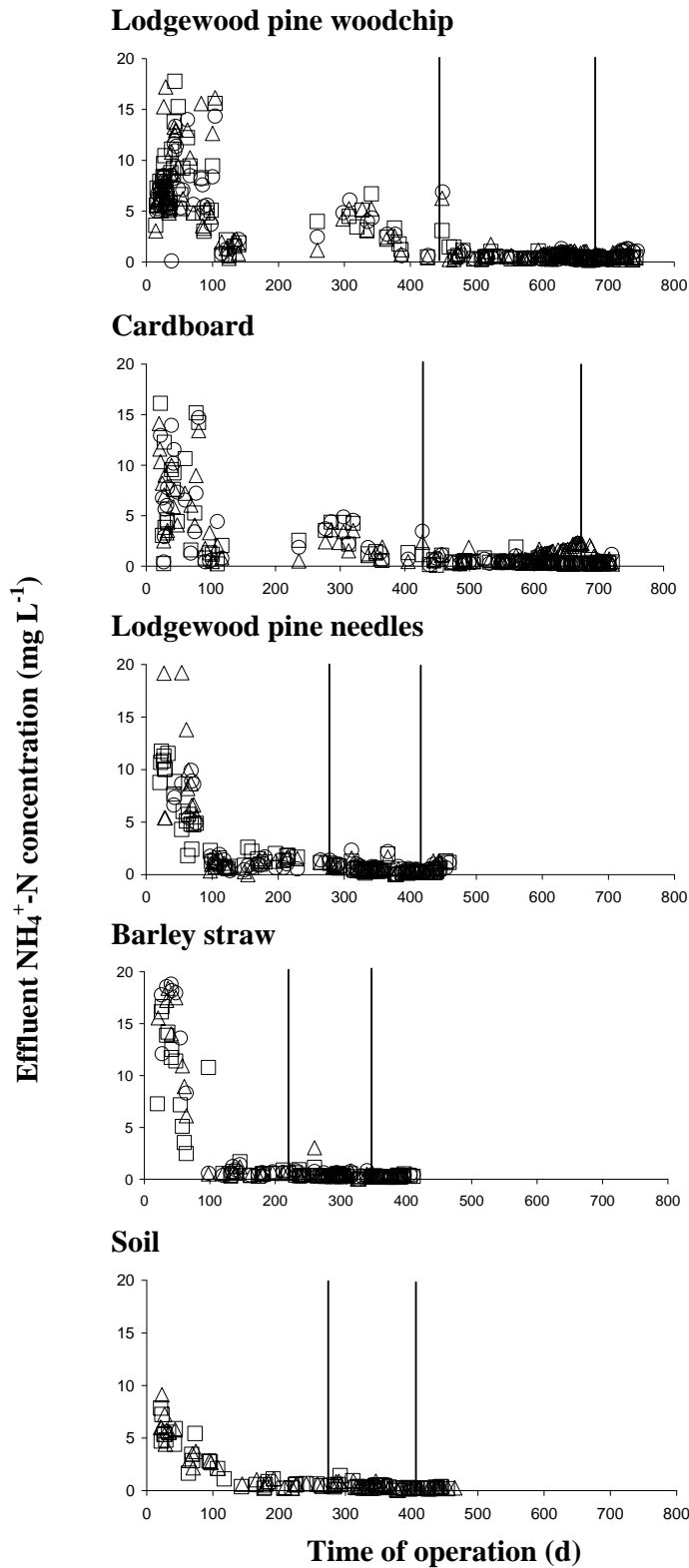
Hydraulic loading rate: 10 cm d⁻¹



- ◆ Lodgewood pine woodchip
- Cardboard
- × Lodgewood pine needles
- ◇ Barley straw
- △ Soil only

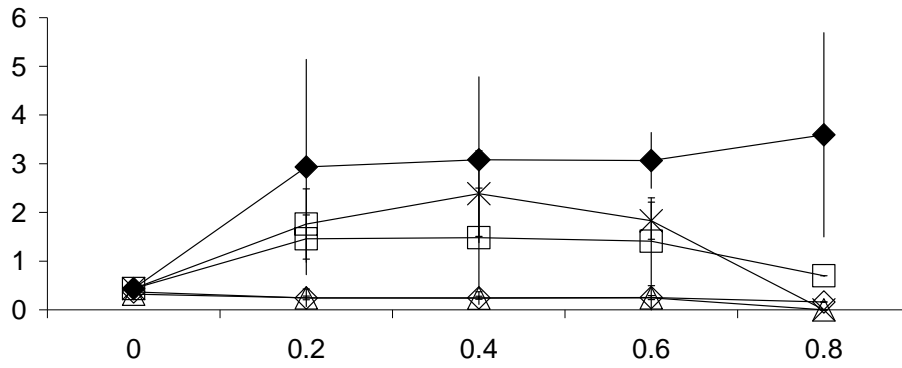
863
864
865
866
867

Figure 5. Average concentration of nitrate in one representative bioreactor containing each media during operation at hydraulic loading rates of 3, 5 and 10 cm d⁻¹.

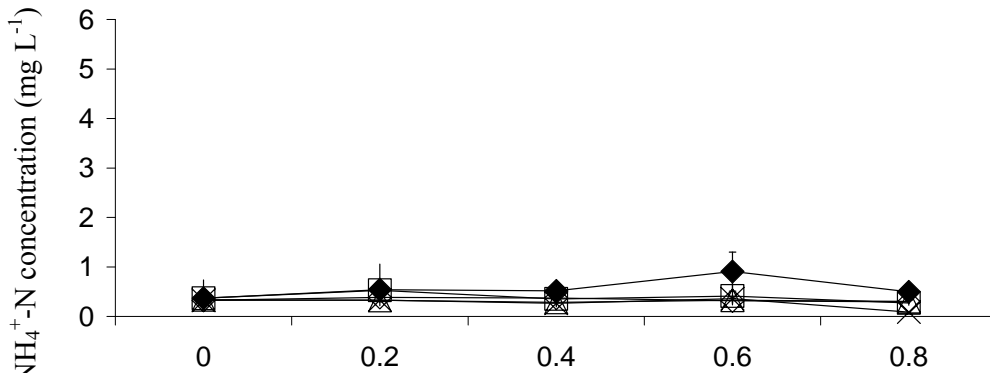


868 Figure 6. Effluent ammonium-N concentrations and operation boundaries for each
 869 media. Open square = Column 1; Open triangle = Column 2; Open circle = Column
 870 3. Vertical lines represent the three hydraulic loading rates: 3, 5 and 10 cm d⁻¹.
 871
 872

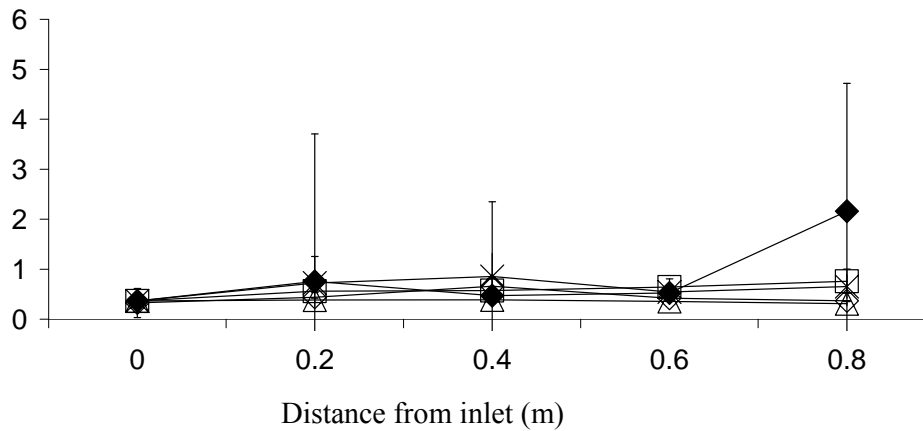
Hydraulic loading rate: 3 cm d⁻¹



Hydraulic loading rate: 5 cm d⁻¹



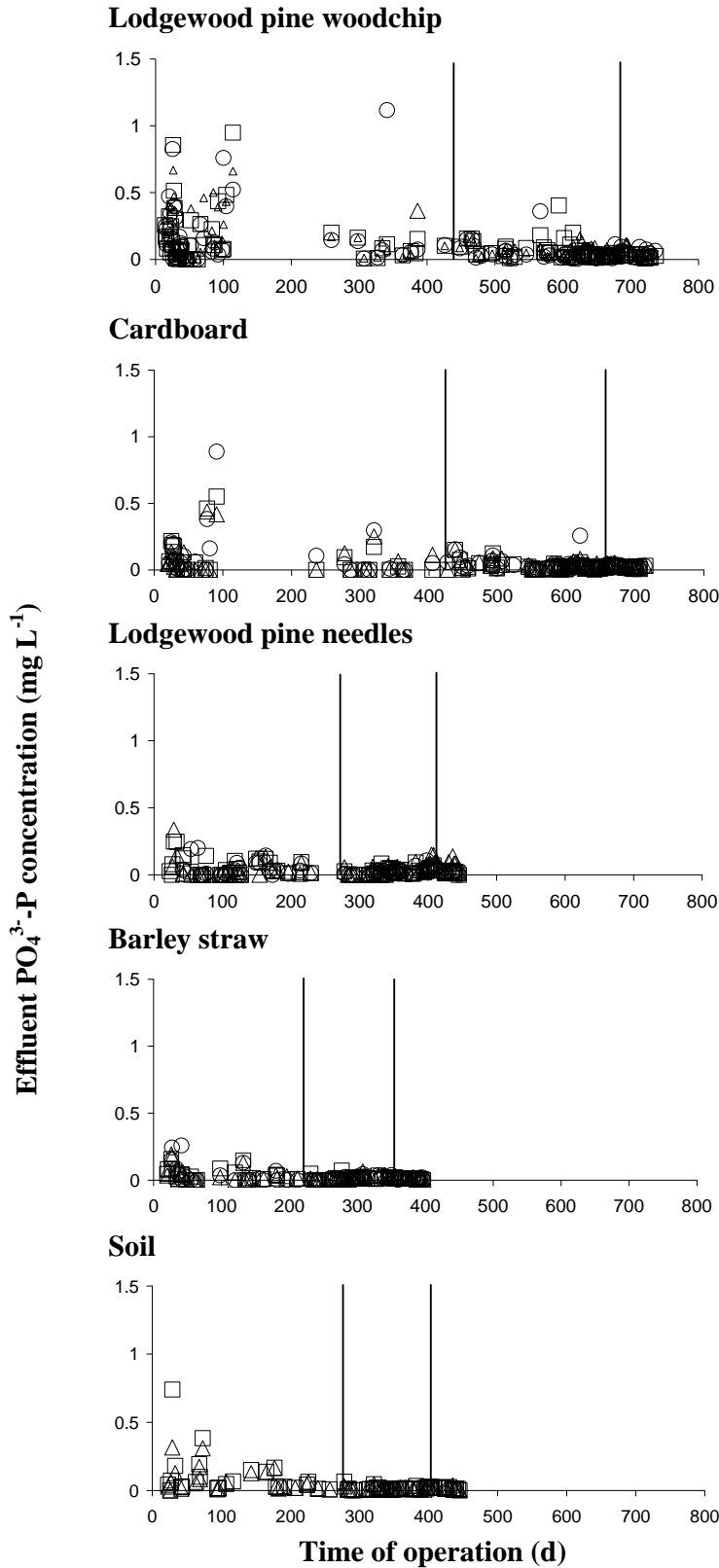
Hydraulic loading rate: 10 cm d⁻¹



- ◆ Lodgewood pine woodchip
- Cardboard
- × Lodgewood pine needles
- ◇ Barley straw
- △ Soil only

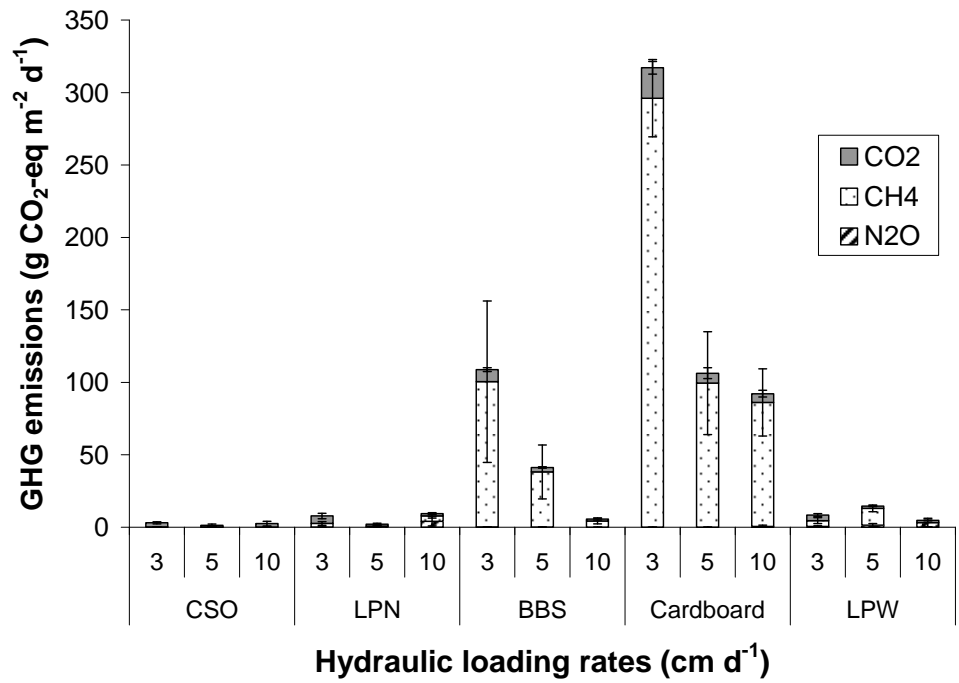
873
874
875
876
877

Figure 7. Average concentration of ammonium-N in one representative bioreactor containing each media during operation at hydraulic loading rates of 3, 5 and 10 cm d⁻¹.



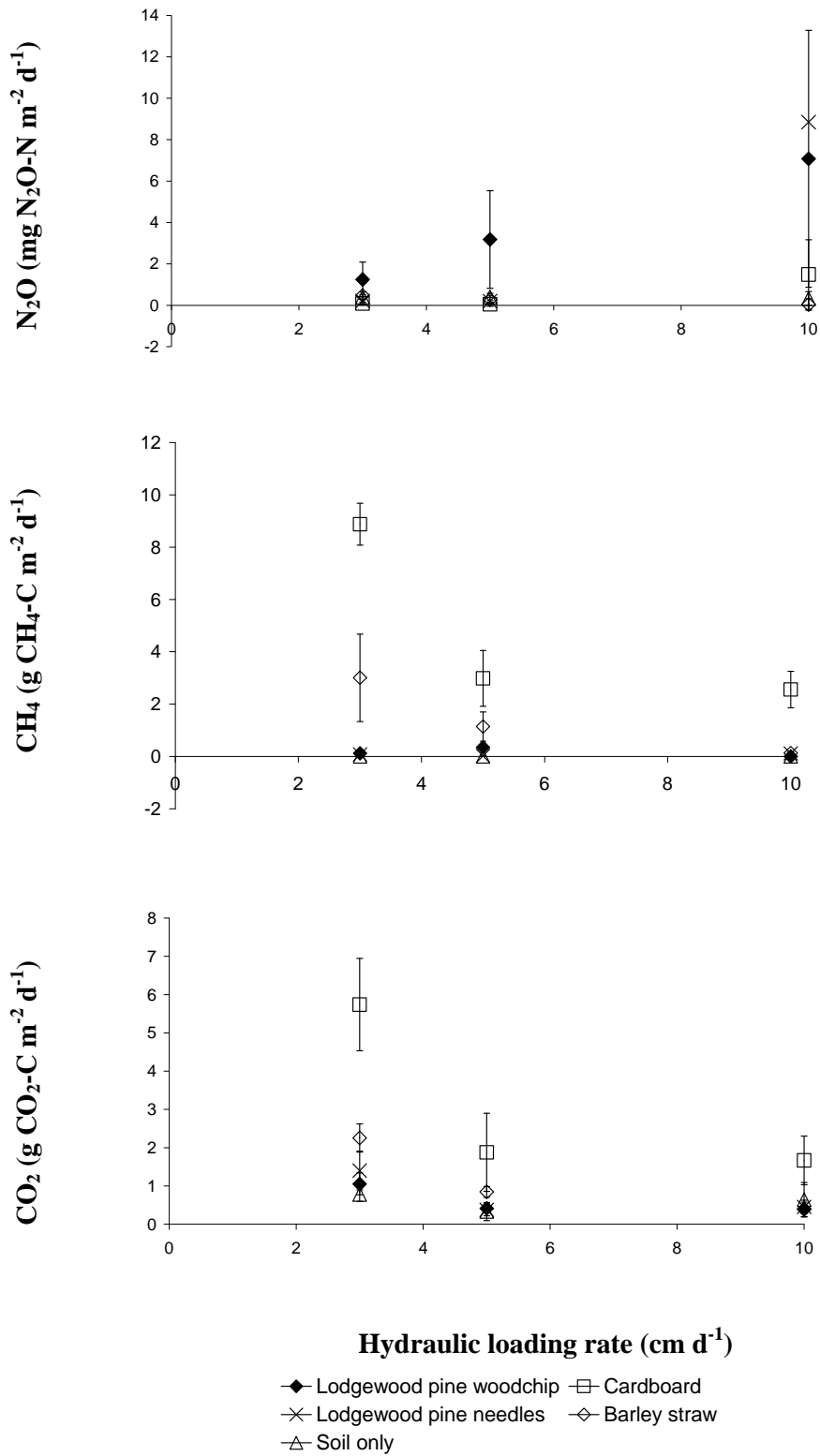
879 Figure 8. Effluent ortho-phosphorus concentration and operation boundaries for each media. Open
 880 square = Column 1; Open triangle = Column 2; Open circle = Column 3. Vertical lines represent the
 881 three hydraulic loading rates: 3, 5 and 10 cm d⁻¹.

882
883
884



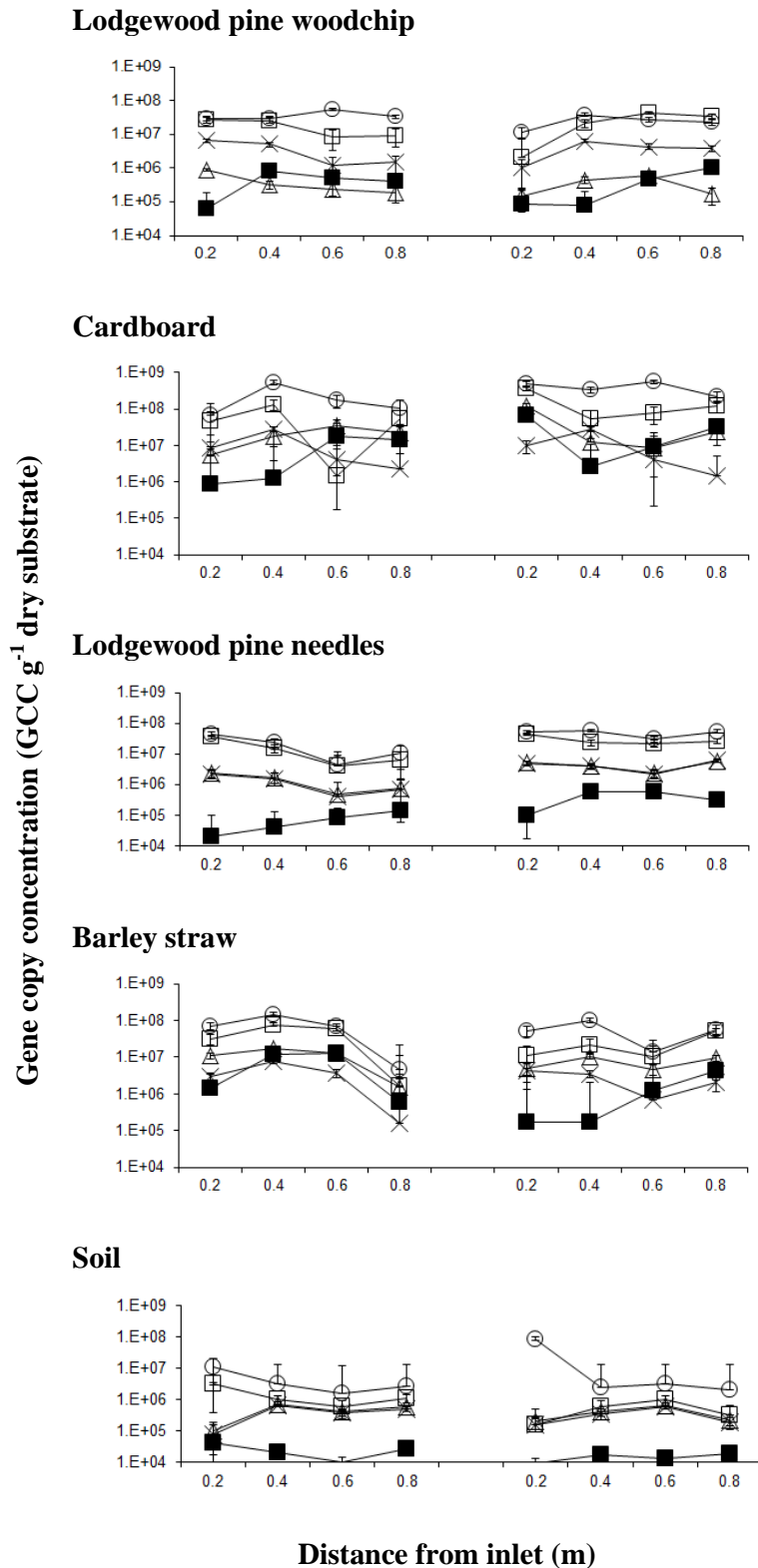
885
886
887
888
889
890
891
892
893
894
895
896
897
898
899
900
901
902
903
904
905
906
907
908
909
910
911
912

Figure 9. Mean emissions of greenhouse gas (nitrous oxide (N₂O), methane (CH₄) and carbon dioxide (CO₂)) emissions (± standard error), expressed as CO₂ equivalents per unit surface area per day.



914
915
916
917

Figure 10. Relationship between hydraulic loading rate and emissions (\pm standard error) in the denitrifying bioreactors.



918 **Figure 11.** Variation in gene copy concentration (GCC) of *nirK* (open triangle), *nirS* (open square),
 919 *nosZ* (cross hairs) and archaeal (closed square) and bacterial 16S rRNA (open circle) obtained from
 920 sampling ports located at distances of 0.2, 0.4, 0.6 and 0.8 m from the base in two arbitrary sets of
 921 lodgewood pine woodchip, cardboard, lodgepole pine needles, barley straw and soil-only bioreactors
 922 (NTC undetected for each respective assay). Standard errors are indicated for each separate Q-PCR
 923 subgroup (n = 3).

